

## SHEAR CAPACITY FOR FULL-SCALE PRECAST CONCRETE PILE

Hidekazu Watanabe<sup>1</sup>, Tomohisa Mukai<sup>1</sup>, Susumu Kono<sup>2</sup>, Taiga Ohtaki<sup>2</sup>, Shinji Kishida<sup>3</sup>, Osamu Kaneko<sup>4</sup>,  
Takeshi Fukuda<sup>5</sup>, Yoshinobu Kiya<sup>6</sup>, Yasuyuki Imai<sup>7</sup>

Building Research Institute, National Research and Development Agency<sup>1</sup>, Tokyo Institute of Technology<sup>2</sup>, Shibaura Institute of Technology<sup>3</sup>, Hiroshima Institute of Technology<sup>4</sup>, Toda Corporation<sup>5</sup>, Concrete Pile Installation Technology Association<sup>6</sup>, Taishingui-kyokai<sup>7</sup>  
Tsukuba<sup>1</sup>; Yokohama<sup>2</sup>; Tokyo<sup>3,5,6,7</sup>; Hiroshima<sup>4</sup>, Japan

### Abstract

In Japan, deep foundation system with precast concrete piles and pile cap is often designed in buildings such as government buildings and residential buildings. In the 2011 Tohoku Earthquake, the pre-cast concrete piles in some buildings were heavily damaged. Some buildings were tilted due to the pile damage. Therefore, it was difficult that these buildings were used continuously after the earthquake. It is important to evaluate capacity of precast concrete pile for considering about post-earthquake functional use. In 2017, Guidelines for Seismic design of reinforced concrete foundation members (draft) was published by Architectural Institute of Japan. Evaluation formulae for shear capacity for precast concrete pile was shown in the guidelines. However, the formulae do not cover the cases of piles under high compressive axial force or tensile axial force. In order to evaluate the shear capacity of precast concrete pile, static loading test was conducted using nine precast concrete pile specimens. The specimens were applied high compressive axial force or tensile axial force. In the result, failure modes of all specimens were classified as shear failure and failure with axial cracks. The failure with axial cracks is not covered the existing formulae. In this study, the failure with axial cracks was observed in the case of piles under compressive axial force.

### Introduction

In Japan, deep foundation system with precast concrete piles and pile cap is often designed in buildings such as government buildings and residential buildings. Under Japanese law, the precast concrete pile is designed based on the allowable stress concept in Japan, generally. Design flow of structural design for pile is shown as follows.

1. Elastic frame analysis for superstructure of the buildings is conducted using static earthquake load (base shear factor 0.2).
2. Design loads of a pile (shear load and axial load) are determined by the elastic frame analysis.
3. Geomaterial properties are measured by geotechnical investigation.
4. Elastic analysis for a pile is conducted using the design loads and the geomaterial property. Generally, Chang's formulae (Chang (1937)) or Broms's formulae (Broms (1964)) are used as elastic analysis for pile.

In the 2011 Tohoku Earthquake, the pre-cast concrete piles in some buildings were heavily damaged. Kaneko (2014) reports some buildings were tilted due to the pile damage. Therefore, it was difficult that these buildings were used continuously after the earthquake. It is important to evaluate capacity of precast concrete pile for considering about post-earthquake functional use. In 2017, Guidelines for Seismic design of reinforced concrete foundation members (draft) (hereafter, AIJ guidelines) was published by Architectural Institute of Japan. Evaluation formulae for shear capacity for precast concrete pile was shown in the AIJ guidelines. However, the formulae do not cover the cases of piles under high compressive axial force or tensile axial force. In order to evaluate the shear capacity of precast concrete

pile, static loading test was conducted using nine precast concrete pile specimens. The specimens were applied high compressive axial force or tensile axial force.

**Specimen details.** Nine specimens in Table 1 were tested. They are full-scale precast concrete piles and prestressed by Prestressing bars. Figure 1 shows reinforcement details. All specimens have hollow section and high strength spun concrete casted using centrifugal method. Specified compressive strength of the concrete is 105 MPa. In this study, two type piles were tested. One type is the Pretensioned spun High strength Concrete pile (hereafter, PHC pile), and another type is Pretensioned and Reinforced spun high strength Concrete Pile (hereafter, PRC pile).

Three PHC piles have same reinforcement details; diameter of the piles is 400mm; length of the piles is 8m; specified thickness of the piles is 65mm. Prestressing bars (10-φ11.2) and spiral hoop (φ3.2@100) are placed in the piles. Specified effective prestressing stress of the piles is 10 MPa. PHC piles were applied different level axial force. PHC18, PHC19 and PHC20 were applied tensile axial force (-344kN), compressive axial force (1368kN) and high compressive axial force (2752kN), respectively.

Six PRC piles have same reinforcement details; diameter of the piles is 400mm; length of the piles is 8m; specified thickness of the piles is 70mm. Prestressing bars (8-φ10) and spiral hoop (φ6.5@70) are placed in the piles. Specified effective prestressing stress of the piles is 5.3 MPa. Shear span ratio of the PRC piles are difference as shown in Table 1. The six PRC piles were applied different level axial force. PRC24 and PRC27 were applied tensile axial force (-196kN and -510kN, respectively). PRC25 and PRC28 were applied compressive axial force (1655kN). PRC26 and PRC29 were applied high compressive axial force (2731kN and 4137kN, respectively).

**Table 1. Specifications of the Specimens**

Concrete		PHC18	PHC19	PHC20	PRC24	PRC25	PRC26	PRC27	PRC28	PRC29
Pile type		PHC pile			PRC pile					
Diameter <i>D</i>	[mm]	400								
Specified thickness	[mm]	65			70					
Actual thickness <i>t</i>	[mm]	76.1	77.3	75.5	81.2	80.7	83.4	80.6	83.4	83.7
Prestressing bar		10-Φ11.2			8-Φ10					
Longitudinal mild reinforcement		-			8-D22					
Spiral hoop		Φ3.2@100			Φ6.5@70					
Shear span ratio		1.4			2.1			1.4		
Specified effective prestressing stress	[MPa]	10			5.3					
Actual effective prestressing force <i>N<sub>e</sub></i>	[kN]	789	794	786	512	515	518	520	516	518
Actual effective prestressing stress <i>σ<sub>e</sub></i> <sup>*1</sup>	[MPa]	10.3	10.3	10.3	6.6	6.7	6.5	6.7	6.5	6.5
Axial Force <i>N</i>	[kN]	-344	1368	2752	-196	1655	2731	-510	1655	4137
Axial stress <i>σ<sub>0</sub></i> <sup>*2</sup>	[MPa]	-4.3	16.8	34.5	-2.1	18	28.8	-5.6	17.5	43.7
Axial Force ratio <i>(N+N<sub>e</sub>)/N<sub>0</sub></i> <sup>*3</sup>		0.04	0.19	0.32	0.03	0.18	0.27	0.00	0.17	0.36

$$*1 \sigma_e = N_e / (A - A_p - A_{pd})$$

$$*2 \sigma_0 = N / \left\{ A + \left( \frac{E_p}{E_c} - 1 \right) A_p + \left( \frac{E_d}{E_c} - 1 \right) A_{pd} \right\}$$

$$*_3 N_0 = \begin{cases} f'_c(A - A_p - A_d) + f_{py}A_p + f_{dy}A_d & (N + N_e > 0) \\ f_{py}A_p + f_{dy}A_d & (N + N_e \leq 0) \end{cases}$$

where,  $A$ : section area,  $A_p$ : total area of prestressing bars,  $A_d$ : total area of longitudinal mild reinforcement,  $E_p$ : Young's modulus of prestressing bars,  $E_d$ : Young's modulus of longitudinal mild reinforcement,  $E_c$ : Young's modulus of concrete,  $f_{py}$ : Yield stress of prestressing bars,  $f_{dy}$ : Yield stress of longitudinal mild reinforcement,  $f'_c$ : concrete compressive strength

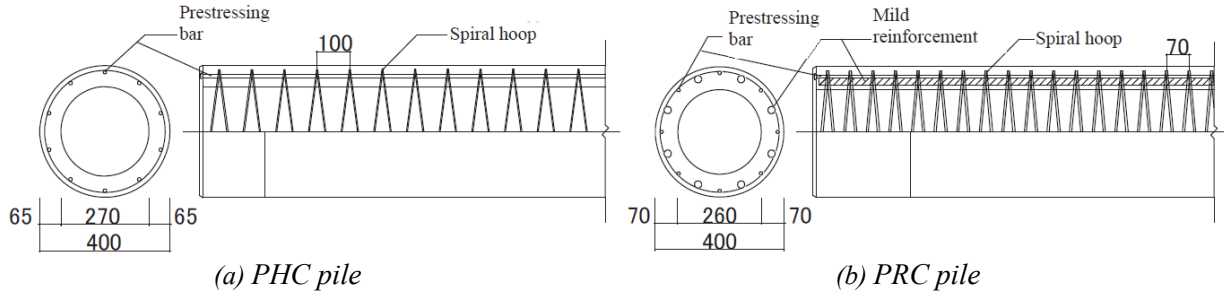


Figure 1. Reinforcement details.

**Table 2. Material Properties**

(a) Steel

Steel		Yield stress [MPa]	Tensile strength [MPa]	Young's modulus [GPa]
Prestressing bar	Φ 10	1360	1431	199
	Φ 11.2	1323	1439	198
Spiral hoop	Φ 3.2	631	695	148
	Φ 6.5	597	649	186
Longitudinal mild reinforcement	D22	387	563	190

(b) Concrete

Concrete	PHC18	PHC19	PHC20	PRC24	PRC25	PRC26	PRC27	PRC28	PRC29
Compressive strength $f_c$ [MPa]	116	117	114	119	127	121	124	132	129
strain at $f_c$ [ $\mu$ ]	2323	2403	2304	2398	2519	2564	2411	2688	2658
Splitting tensile strength [MPa]	5.1	5.2	5.5	6.5	8.5	8.6	8.6	7.8	8.0
Young's modulus [GPa]	49.1	48.7	50.4	49.6	50.4	47.2	51.4	49.1	48.5

**Test setup.** The experimental test was conducted in large size structure laboratory, Building Research Institute. Loading system and test setup is shown in Figure 2. As shown in Figure 2, the loading system consisted of four horizontal hydraulic jacks, two vertical hydraulic jacks, two support point and loading frame. Axial load of specimens was applied by four horizontal hydraulic jacks. Shear force of specimens was applied by two vertical hydraulic jacks at the center. The two jacks were controlled to work inverse direction, each other. Therefore, moment distribution of specimens is illustrated in Figure 3. Span of two vertical hydraulic jacks ( $=l$ ) is 1.0m (PHC piles and PRC24-26) or 1.5m (PRC27-29). The center range between vertical hydraulic jacks is test area in this study. The loading is displacement -controlled with control drift angle  $R$ . The control drift angle  $R$  is calculated as Equation (1).

$$R = (\delta_{+175} - \delta_{-175})/(l + 175 \times 2) \quad (1)$$

where,  $\delta_{+175}, \delta_{-175}$ : displacement measured by displacement gauge placed 175mm outside of the test area as shown in Figure 3.

The loading protocol consisted of two cycles at drift angle  $R=0.125\%, 0.25\%, 0.5\%, 1.0\%, 1.5\%, 2.0\%, 3.0\%, 4.0\%$ . Loading test stopped when specimen was unable to keep axial force or when the specimen strength dropped to 80% of the maximum shear force. During loading test, loading frame was hanged by four hanging hydraulic jacks for canceling gravity load of loading frame.

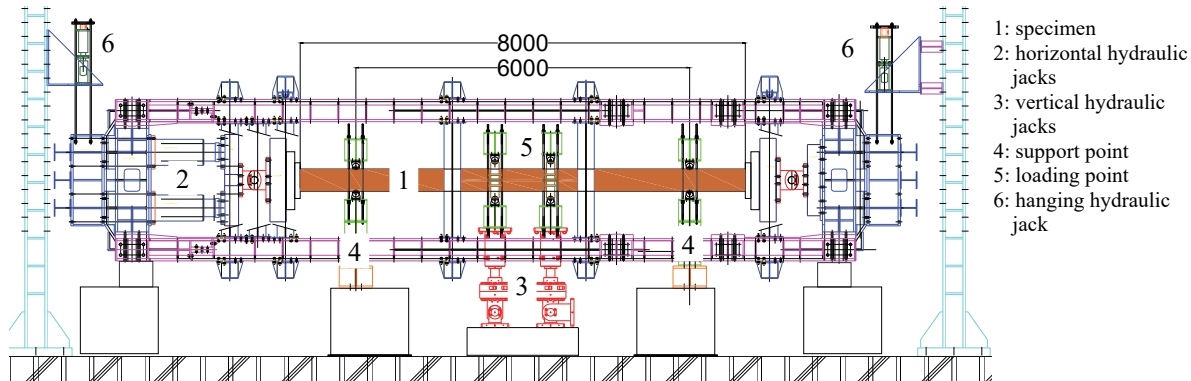


Figure 2. Test setup (unit: mm).

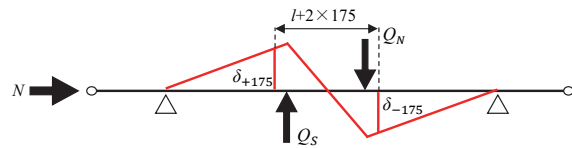


Figure 3. Moment distribution for specimens.

**Experimental results.** The experimental results are summarized in Table 3. Figure 4 shows shear force ( $Q$ ) - control drift angle ( $R$ ) responses. Important response points (shear cracking, spiral hoop tensile yielding, prestressing bar tensile yielding, longitudinal mild reinforcement tensile/compressive yielding, the maximum shear force) are plotted. Shear force  $Q$  is calculated considering  $P-\Delta$  effect by axial load of specimens. In this study, failure mode of specimen is classified as shear failure (S), shear failure after yielding (YS), failure with axial crack (A). In the case of shear failure and shear failure after yielding, capacity of specimen is determined due to diagonal crack. On the other hand, in the case of failure with axial crack, it is determined due to axial crack.

- PHC18, PRC24 and PRC27 (under tensile axial force)

For PHC18, shear cracks were observed during the first cycle to  $R=0.25\%$ . Spiral hoop tensile yielding was observed during the first cycle to  $R=0.5\%$ . After that, PHC18 reached the maximum shear force at the first cycle at same cycle. After the test, spiral hoop fracture was observed. For PRC24 and PRC27, shear cracks and spiral hoop tensile yielding were observed. The number of shear cracks was increased with increase of control drift angle. Prestressing bar tensile yielding was observed during the first cycle to  $R=1.0\%$ . After that, PRC24 and PRC27 reached the maximum shear force at the first cycle at the first cycle to  $R=1.5\%$ . During loading test, PHC18, PRC24 and PRC27 kept constant axial force.

- PHC19, PRC25 and PRC28 (under compressive axial force)

For PHC19, shear cracks, axial cracks and spiral hoop tensile yielding were observed during the first cycle to  $R=0.5\%$ . PHC19 reached the maximum shear force at the same cycle. During the first cycle to  $R=0.75\%$ , spiral hoop was fractured suddenly, at the same time, the specimen was crashed and unable to keep axial force. For PRC25 and PRC28, shear cracks and spiral hoop tensile yielding were observed. The number of shear cracks was increased with increase of control drift angle as shown in Figure 5. After

that, PRC25 and PRC28 reached the maximum shear force at the first cycle at the first cycle to R=0.75% and R=0.5%, respectively. During loading test, PRC25 and PRC28 kept constant axial force.

- PHC20, PRC26 and PRC29 (under high compressive axial force)

For PHC20, axial cracks and spiral hoop tensile yielding were observed during the first cycle to R=0.5% as shown in Figure 6 (a). During the first cycle to R=0.75%, spiral hoop was fractured suddenly, furthermore, the specimen was crashed and unable to keep axial force as shown in Figure 6 (b). PHC20 reached the maximum shear force at the same time. For PRC26, shear cracks and axial cracks were observed during the first cycle to R=0.5%. PRC19 reached the maximum shear force at the same cycle. During loading test, PRC26 kept constant axial force. For PRC29, axial cracks and spiral hoop tensile yielding were observed during the first cycle to R=0.5%. PRC29 reached the maximum shear force at the same cycle. During the first cycle to R=0.75%, spiral hoop was fractured suddenly, at the same time, the specimen was crashed and unable to keep axial force.

**Table 3. Test Results**

			PHC18	PHC19	PHC20	PRC24	PRC25	PRC26	PRC27	PRC28	PRC29
Axial Force ratio $(N+N_e)/N_0$			0.04	0.19	0.32	0.03	0.18	0.27	0.00	0.17	0.36
Failure mode *			S	A	A	YS	S	A	YS	S	A
Shear Cracking	Pos.	Q [kN]	207.4	372	397.1	222.4	373.7	-	219.3	437	-
		R* (%)	0.2	0.31	0.29	0.328	0.372	-	0.418	0.291	-
	Neg.	Q [kN]	-183.8	-333.5	-	-213.8	-459.3	-407.1	-193.8	-356	391.6
		R* (%)	-0.18	-0.24	-	-0.388	-0.493	-0.399	-0.304	-0.276	-0.319
Spiral hoop tensile yielding	Pos.	Q [kN]	241.6	372	442	-	-	-	404.1	536	563.3
		R* (%)	0.416	0.31	0.433	-	-	-	1.062	0.417	0.359
	Neg.	Q [kN]	-	-	-	-216.7	-413.1	-305.8	-	-	-
		R* (%)	-	-	-	-0.393	-0.396	-0.964	-	-	-
Prestressing bar tensile yielding	Pos.	Q [kN]	-	-	-	326.7	-	-	379.7	-	-
		R* (%)	-	-	-	0.705	-	-	0.932	-	-
	Neg.	Q [kN]	-	-	-	-288.8	-	-	-291.7	-	-
		R* (%)	-	-	-	-0.683	-	-	-0.675	-	-
Longitudinal mild reinforcement tensile yielding	Pos.	Q [kN]	-	-	-	297.6	-	-	420.4	-	-
		R* (%)	-	-	-	0.6	-	-	1.147	-	-
	Neg.	Q [kN]	-	-	-	-	-	-	-	-	-
		R* (%)	-	-	-	-	-	-	-	-	-
Longitudinal mild reinforcement compressive yielding	Pos.	Q [kN]	-	-	-	-	254.8	-	-	373	447.5
		R* (%)	-	-	-	-	1.382	-	-	1.071	0.257
	Neg.	Q [kN]	-	-	-	-	-	481.9	-	-	-357.7
		R* (%)	-	-	-	-	-	0.716	-	-	-0.276
The maximum shear force	Pos.	Q [kN]	247.6	420.6	467.5	433.1	525.5	508.7	464.1	627	671
		R* (%)	0.518	0.498	0.726	1.564	0.76	0.499	1.453	0.584	0.502
	Neg.	Q [kN]	-198.5	-337.4	-326.8	-382.8	-482.6	-453.9	-424.8	-517	-547.9
		R* (%)	-0.269	-0.257	-0.255	-1.484	-0.757	-0.505	-1.491	-0.518	-0.509

\* S: Shear failure, YS: Shear failure after yielding, A: Failure with axial crack

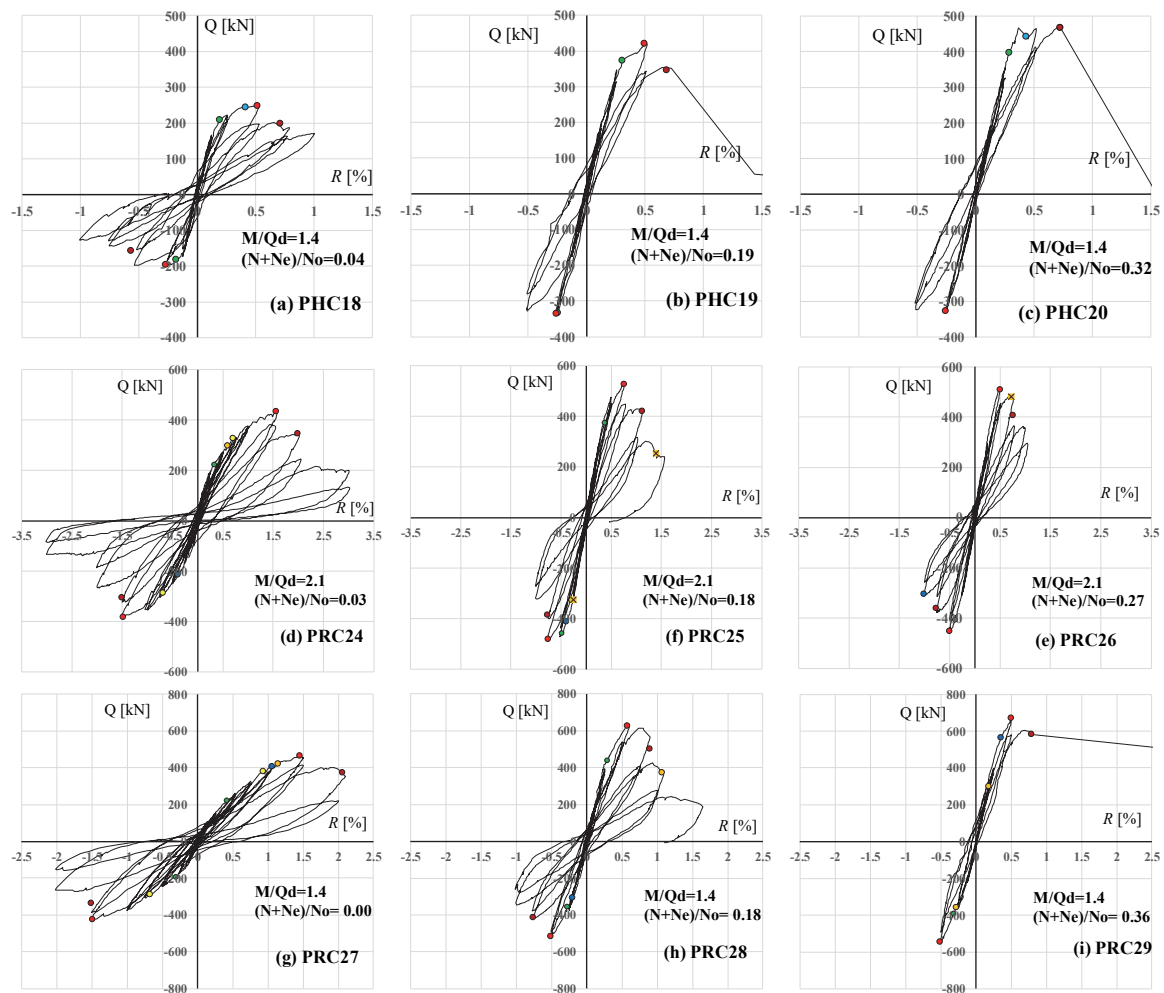


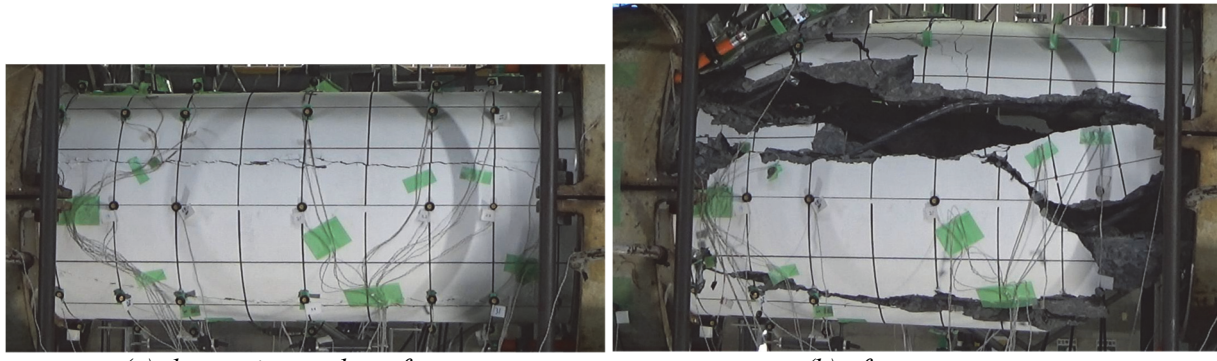
Figure 4. Shear force versus drift angle relations.



(a) the maximum shear force

(b) after test

Figure 5. damage of Specimen PRC28.



(a) the maximum shear force

(b) after test

Figure 6. damage of Specimen PHC20.

**Evaluation of shear capacity for specimens.** Evaluation formulae for shear capacity for precast concrete pile was shown in AIJ guidelines. The existing formulae for PHC pile and PRC pile are shown in Equation (2) and (3), respectively. However, the formulae do not cover the cases of piles under high compressive axial force or tensile axial force. Equation (2) covers only Axial stress range are from 0MPa to 30MPa. On the other hand, Equation (3) covers only Axial stress range are from 0MPa to 5MPa. Thus, all specimens except PHC19 are not covered the existing formulae. Comparison of test results and calculation results are shown in Figure 7. The calculation results were calculated using Equation (2) or (3). In the case of shear failure and shear failure after yielding, the existing formulae underestimated the shear capacity of test results. However, In the case of failure with axial crack, the existing formulae overestimated the shear capacity of test results. The existing formulae was developed for shear failure; thus, it is difficult to evaluate shear capacity for different failure mode.

$$Q_{cal1} = \alpha \cdot \eta \cdot \frac{t \cdot I}{S_0} \cdot \sqrt{(\sigma_g + 2\sigma_d)^2 - \sigma_g^2} \quad (1)$$

$$Q_{cal2} = \left[ \frac{0.092k_u k_p(18+f_c)}{M/(Q \cdot d) + 0.12} + 0.85\sqrt{P_w \sigma_{wy}} + 0.1(\sigma_0 + \sigma_e) \right] b j \quad (2)$$

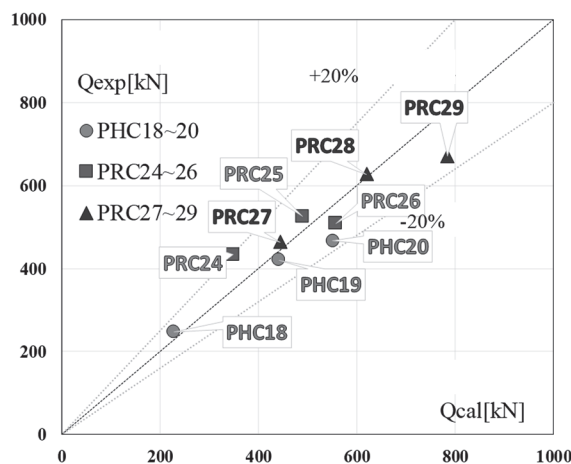


Figure 7. comparison of test results and calculation.

**Table 4. Evaluation of Shear Capacity**

		PHC18	PHC19	PHC20	PRC24	PRC25	PRC26	PRC27	PRC28	PRC29	
Axial stress $\sigma_0$ Failure mode		[MPa]	-4.3 S	16.8 A	34.5 A	-2.1 YS	18 S	28.8 A	-5.6 YS	17.5 S	43.7 A
shear capacity	$Q_{exp}$	[kN]	247.6	420.6	467.5	433.1	525.5	508.7	464.1	627	671
	$Q_{cal}$	[kN]	228	442	551	349	490	557	445	620	784
	$Q_{exp}/Q_{cal}$		1.09	0.95	0.85	1.24	1.07	0.91	1.04	1.01	0.86

## Conclusions

Loading test on nine precast concrete pile specimens was carried out to evaluate shear capacity. The conclusions drawn from this study are summarized as follows:

- Failure mode of specimens under tensile axial force are shear failure. During loading test, specimens under tensile axial force kept constant axial force. The failure with axial cracks was observed in the case of specimens under compressive axial force.
- In the case of shear failure and shear failure after yielding, the existing formulae underestimated the shear capacity of test results. However, In the case of failure with axial crack, the existing formulae overestimated the shear capacity of test results. The existing formulae was developed for shear failure; thus, it is difficult to evaluate shear capacity for different failure mode.

## Acknowledgment

The research was funded by R&D Subjects “Development on performance based seismic design for government office buildings and evacuation facilities with post-earthquake functional use” by Building Research Institute. The research was supported by grant-in-aid for research of Ministry of Land, Infrastructure and Transport, Japan.

## References

- Chang, Y. L., 1937, “Discussion on lateral pile-loading test by Feagin,” ASCE, pp. 272-278.
- Broms, B. B., 1964, “Lateral resistance of piles in cohesive soils,” *Soil Mechanics and Foundation Division*, ASCE, pp. 27-63.
- Kaneko, O., 2014, “Situations and Analysis of Damage to Pile Foundations of Buildings in 2011 Great East Japan Earthquake,” The Japanese Geotechnical Society, vol.62, No.1, pp. 16-19. (in Japanese)
- Architectural Institute of Japan, 2017, “Guidelines for Seismic design of reinforced concrete foundation members (draft),” AIJ. (in Japanese)